



Effects of structure design on electrostatic pull-in voltage of perforated nanoswitch with intermolecular surface forces

Rachid Kerid^{*1}, Younes Bounnah²

¹Institute of Electronics, University of Blida 1, BP. 270 09000, Algeria;

²High School of Hydraulics, Algeria;

^{1,2}MVRE Laboratory, ENSH of Blida, Algeria.

Received: 21 May 2021; Accepted: 11 October 2021

*Corresponding author email: r.kerid@ensh.dz

ABSTRACT

In this paper, we model and investigate the electrostatic pull-in instability of a perforated cantilever nanoswitch subjected to van der Waals and Casimir forces. The nanocantilever is a beam structure perforated with a periodic square holes network, which has been considered as an electrode material for this new structure. Closed-form solutions for the critical pull-in parameters are derived from the standard deformation beam equation, in which an equivalent bending stiffness is considered due to presence of square holes network. The electrostatic and dispersion forces are included by modifying the standard deformation beam equation, while the small scale effect is introduced by using the Eringen's nonlocal elasticity theory. Pull-in parameters analysis of the perforated nanoswitch indicated that both pull-in voltage and pull-in deflection are affected by the gap ratio as well as the hole size ratio and the number of holes along the section of perforated nanocantilever beam. Therefore, these results are compared with literature results where new remarks are deduced and presented with detailed discussion for a proper design and investigation of M/NEMS nanoswitches.

Keywords: *Cantilever nanoswitch, Pull-in instability, Periodic square holes, Equivalent parameters, Nonlocal parameter*

1. INTRODUCTION

Nanobeam structures have been widely used as common mechanical components based electrostatic nanoswitch devices integrated in micro/nanoelectromechanical systems (M/NEMS) [1-6] for switching applications with reduced size and low cost. A typical electrostatic nanoswitch is a fundamental building block composed of two parallel nanobeams, one is fixed and the other is movable, which can be actuated electrically and a dielectric spacer separating the two electrodes, the movable electrode deflects towards the ground electrode due to the electrostatic force and intermolecular interactions. When the voltage increases above a critical value, the cantilever

beam becomes unstable and pulls-in onto the fixed electrode. Such as this phenomenon is called "the pull-in instability" that plays an important role for the design step of electrostatic nanoswitch devices [7-11].

Several researches have focused on the electromechanical interaction modeling to estimate the pull-in parameters for electrostatic nanoswitch, in which various mechanical deflection models have been proposed by authors. Osterberg and Senturia [12] found an analytical expression for the determination of pull-in parameters of MEMS switches based on the classical elasticity theory of material. Bochobza-Degani and Nemirovsky [13] presented a lumped two degrees of freedom model

for a direct calculation of the pull-in parameters under electrostatic actuators actuation. Also, the reduction of the separation between the components of cantilever switch was studied in refs. [14-16]. However, when the separation is below 20 nm, the van der Waals force is operational and thus should be considered in the deformation beam equation as an additive term. A theoretical study was proposed by Ramezani et al. [7] to investigate the effect of the van der Waals force on the pull-in parameters of nanoswitches where noticeable conclusions were deduced from numerical results. On the other hand, the Casimir force effect can affect the electromechanical nanoswitch behavior at separation above 20 nm [11], and again an additive term should be introduced in the deformation beam equation for a proper numerical computation. Including the Casimir effect on the electromechanical nanoswitch model, a computation of the pull-in gap and pull-in voltage of NEMS switch was carried out by Lin and Zhao to investigate the Casimir force effect on the linear [3, 4] and nonlinear [5] behavior of a nanoscale electrostatic actuator.

Nevertheless, according to the experimental verifications and numerical simulations [17-18], the evaluation of the electromechanical behavior using the classical elasticity theory remains unable due to the presence of the small scale effects at nanometric dimensions [19]. Unlike the classical elasticity theory, Eringen's nonlocal elasticity theory of material [20-24] is a scale dependent theory accounts the small scale effects. Using this theory, several studies [25- 32] have investigated the small scale effect on the pull-in instability of nanoswitches.

Nowadays, perforation is a geometric procedure widely used in advanced technologies to develop sensitive structures especially for optomechanics and photonics [33-39]. Despite the crucial role of perforation in the current technologies, the perforated nanostructures behavior has not been analyzed as extensively as full nanostructures behavior but only for particular cases due to the problem complication. Sharpe et al. [40] investigated the holes size effect on the mechanical characteristics of polysilicon thin film, and they confirmed that the Young's modulus value decrease of 12% and the strength of the holed specimens drops by 50%. Rabinovich et al. [41] investigated the holes size effect on Young's modulus and

shear modulus by studying the electromechanical behavior of a perforated beam structure. Their results showed that Young's modulus and shear modulus are directly affected by holes size with a decrease of 24% and 30% respectively. Luschi and Pieri [42, 43] calculated the equivalent bending stiffness and shear stiffness for perforated structures with periodic square holes network. However, the influence of the periodic square holes network on the pull-in instability of perforated cantilever nanoswitches has not been addressed.

In this work, the influence of a periodic square holes network on the pull-in instability of perforated cantilever nanoswitches under electrostatic and intermolecular forces is studied for varying gap ratio, numbers and sizes of holes using a linear distributed load (LDL) to develop closed-form solutions. The paper is organized as follows: in section 2, theoretical formulation based on nonlocal elasticity is presented. In section 3, closed-form solutions for the critical pull-in parameters are derived from the standard deformation beam equation. Pull-in voltage and deflection are analyzed with numerical calculations and detailed discussions in section 4. Concluding remarks of work are given in section 5.

2. PROBLEM FORMULATION

In this section, the perforated nanobeam will be analyzed in order to investigate the pull-in parameters of the cantilever nanoswitch, we consider a nanobeam of length L , width w and thickness h , with periodic square holes network of spatial period s_p and size of hole d_h . We also define N as the number of holes along the section, and $(\gamma = d_h / s_p)$ as the hole size ratio which can range from 0 (full beam) to 1 [33, 35]. Figure 1 presents the geometry of perforated cantilever nanoswitch structure with periodic square holes network proposed in this paper.

According to Eringen's nonlocal theory [22, 23], the stress-strain relationship for the nanobeam can be given as:

$$\sigma(x) - \mu^2 \frac{d^2 \sigma(x)}{dx^2} = E \varepsilon(x) \quad (1)$$

Where σ and ε are stress and strain, respectively, E is Young's modulus of the beam and $\mu = \mu^* L$ is nonlocal parameter revealing the small-scale effect with $\mu^* \in [0, 0.2]$ as indicated in ref. [52].

The equilibrium of forces in the vertical direction and moments of the beam is given by:

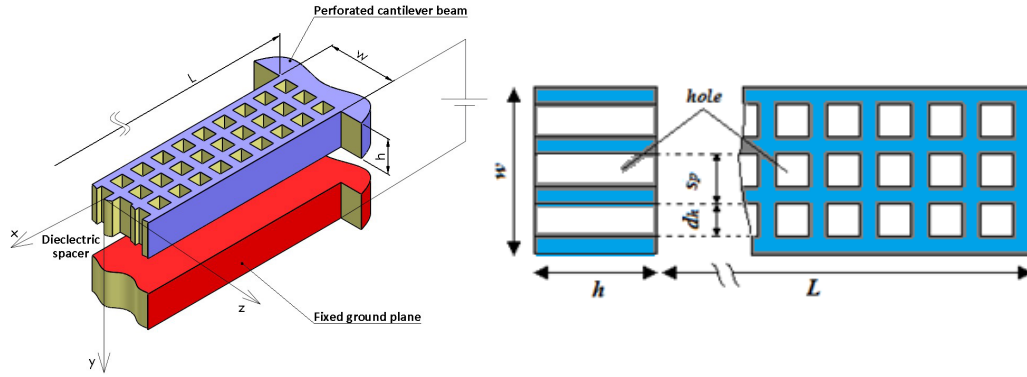


Fig. 1- (a): Schematic representation of a perforated cantilever switch; (b): Part of the total length of the beam is cut away for more clarity.

$$\frac{dQ}{dx} = -F(x), Q = \frac{dM}{dx} \quad (2)$$

Where $F = F_{elec} + F_n$ ($n=3, 4$) is the distributed lateral load per unit length, Q is the transverse shear force and M is the bending moment.

From equation (3) and equation (1) the nonlocal constitutive can be given as

$$M(x) - \mu^2 \frac{d^2 M}{dx^2} = -EI_{eq} \frac{d^2 y}{dx^2} \quad (3)$$

It can be derived from the equations (2) and (3) that the governing equation for the electrostatic deformation of the nano-beam is [20-24].

$$EI_{eq} \frac{d^4 y}{dx^4} = F - \mu^2 \frac{d^2 F}{dx^2} \quad (4)$$

Where y is the deflection the beam, x the position along the beam, and is the EI_{eq} is the equivalent bending moment rigidity of the beam.

Considering the first order fringing field effect, the electrostatic force per unit length of the beam [7, 43, 44] is given by:

$$F_{elec} = \frac{\epsilon_0 w V^2}{2(g-y)^2} \left(1 + 0.65 \frac{(g-y)}{w}\right) \quad (5)$$

where $\epsilon_0 = 8.854 \times 10^{-12} \text{ C}^2 \text{ N}^{-1} \text{ m}^{-2}$ is the permittivity of vacuum, V is the applied voltage, w is the beam width and g is the initial gap between the movable and the ground electrode.

The van der Waals force per unit length of the beam is [15].

$$F_3 = \frac{Aw}{6\pi(g-y)^3} \quad (6)$$

where A is the Hamaker constant.

The casimir force per unit length of the beam is [16].

$$F_4 = \frac{\pi^2 hcw}{240(g-y)^4} \quad (7)$$

where $h = 1.055 \times 10^{-34} \text{ Js}$ is Planck's constant divided by 2π and $c = 2.998 \times 10^8 \text{ ms}^{-1}$ is the speed of light.

To facilitate formulation of the model, the nondimensional form is introduced

$$u = y/g, \rho = x/L \quad (8)$$

The following dimensionless equation is obtained

$$F(\rho) - \mu^2 \frac{d^2 F(\rho)}{d\rho^2} \quad (9)$$

where

$$F(\rho) = \frac{R_n}{(1-u(\rho))^n} + \frac{\beta}{(1-u(\rho))^2} + f \frac{\beta}{(1-u(\rho))} \quad (10)$$

The index n is 3 for the van der Waals force and 4 for the Casimir effect.

$$R_3 = \frac{AwL^4}{6\pi g^4 EI_{eq}}$$

$$R_4 = \frac{\pi^2 hcwL^4}{240g^5 EI_{eq}} \quad (11)$$

$$\beta = \frac{\epsilon_0 w V^2 L^4}{2g^3 EI_{eq}}, f = 0.65 \frac{g}{w}$$

Luschi and Pieri in [42] determined the analytical expressions of equivalent bending stiffness EI_{eq} as function of number of holes N and the filling ratio α . To this purpose, we define the geometric parameters of the beam.

$$\alpha = 1 - \gamma \quad (12)$$

The analytical expression of EI_{eq} has been determined by using Eq. (13). (13)

$$EI_{eq} = \frac{EI_{cb}(N+1)\alpha(N^2+2N+\alpha^2)}{(1-\alpha^2+\alpha^3)N^3+3\alpha N^2+(3+2\alpha-3\alpha^2+\alpha^3)\alpha^2 N+\alpha^3}$$

where E is the Young's modulus, and I_{cb} , the moment of inertia corresponding to a full beam.

3. ELECTROSTATIC PERFORATED CANTILEVER NANOSWITCH

For perforated cantilever switch under electrostatic force, the lateral load $F(\rho)$ is approximated by:

$$F = F_r \rho \tag{14}$$

Replacing this approximation in Eq. (9), we obtain:

$$\frac{d^4 u}{d\rho^4} - F_r \rho = 0 \tag{15}$$

The associated boundary conditions at the fixed end ($\rho = 0$) are:

$$u(0) = \frac{du(0)}{d\rho} = 0 \tag{16}$$

and at the free end ($\rho = 1$), we obtain the deflection curve as:

$$u = \frac{F_r \rho^5}{120} - \frac{F_r(1-2\mu^2)\rho^3}{12} + \frac{F_r \rho^2}{6} = 0 \tag{17}$$

Where the tip deflection $u_r = u(1)$

$$u_r = \frac{F_r(11-20\mu^2)}{120} = 0 \tag{18}$$

From equation (10),

$$F_r = \frac{R_n}{(1-u_r)^n} + \frac{\beta}{(1-u_r)^2} + f \frac{\beta}{(1-u_r)} \tag{19}$$

We obtain relationship between β and u_r

$$\beta = \frac{(11-20\mu^2)}{1} \frac{(1-u_r)^n}{(1-u_r)^2 - \frac{f}{1-u_r}} \tag{20}$$

By deriving $d\beta/du_r=0$ to obtain β_{pi} the pull-in voltage V_{pi} of perforated cantilever nanoswitch can be obtained as follow

$$V_{pi} = \left(\frac{2g^3 EI_{eq} B_{pi}}{\epsilon_0 L^3 Sa} \right)^{1/2} \tag{21}$$

With EI_{eq} , equivalent bending stiffness and Sa is active surface of a perforated nanobeam.

4. FABRICATION PLAN FOR NEMS

The proposed cantilever nanoswitch with embedded contact electrodes can be fabricated using bulk-silicon techniques based on the silicon anodic bonding to form and pattern the mechanical and actuation structures. The fabrication process is summarized as follow:

First, a silicon wafer with a polished surface can be patterned and etched to a depth of 3.5nm. Next, another wafer can be etched to form the dimple for the contact electrode. Then, a SiO₂ insulating layer can be deposited on the silicon device layer and the unexposed region of the SiO₂ layer etched to a depth already determined. Then, the metal layer can be sputtered and patterned by a lift-off process, the SiO₂ layer can be etched to this depth to remove the unexposed region. Next, the same metal layer as in previous step can be sputtered to make the electrodes and leads. After this step, the silicon layer can be anodically bonded to the substrate. Finally, the device layer can be etched by ICP (Inductively Coupled Plasma) to release the nanoswitch structures.

5. RESULTS AND DISCUSSIONS

We investigate the effect of dispersion (van der Waals and Casimir) forces on the pull-in instability of perforated cantilever nanoswitch with length $L=200$ nm, width $w=18$ nm and thickness $h=3.5$ nm. Young modulus $E_0=166$ GPa and the values of nonlocal parameter μ are 0, 0.01 and 0.05. The value of equivalent parameter EI_{eq} is calculated as a function of number of holes N and filling ratio $\alpha=1-\gamma$ by using the analytical expression given in equation (13). In order to validate our results, we compared our model with the LDL model used by Yang et al. [19], the lamped model used by Lin and Zhao [3, 4] and the distributed parameter model used by Ramezani et al. [7].

As can be seen from table 1, the values of pull-in voltage increase with the gap ratio g/w from the minimum value fixed at $g/w=0.9$ to maximum value of voltage V_{pi} located at $g/w=1.2$. As can be observed, the pull-in voltage of a perforated cantilever switch gives good results with respect to the conventional structure. In addition, we found that our results were remarkably similar those predicted by Yang et al. in ref [19]; Ramezani et al. in ref [7] and Lin and Zhao in ref [4]. The nonlocal effect is not considered in this state. Also, an increase of pull-in voltage for results including small scale effect compared with results excluding

Table 1- Comparison of pull-in voltages (in V) with varying g/w for full and perforated switch ($\gamma = 0.9$, $\mu = 0.00$ and $N = 10$)

g/w	van der Waals force				Casimir force			
	[3]	[7]	[19]	Present	[4]	[7]	[19]	Present
0.9	0.8944	1.2329	1.1369	0.6776	0.5015	0.6428	0.6019	0.1449
1.0	1.1705	1.5309	1.4289	0.8089	0.5993	0.7579	0.7120	0.6220
1.1	1.4162	1.8093	1.6981	0.9501	0.6955	0.8728	0.8217	0.9062
1.2	1.6472	2.0785	1.9564	1.1027	0.7915	0.9884	0.9318	1.1632

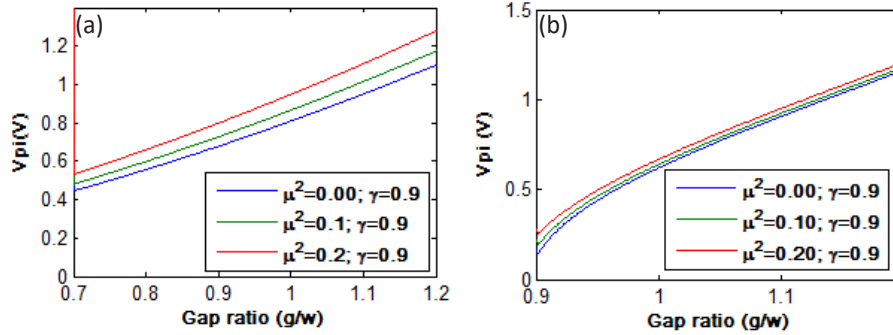


Fig. 2- Effect of gap ratio g/w on the pull-in voltage of perforated cantilever nanoswitch under (a) van der Waals force (b) Casimir force.

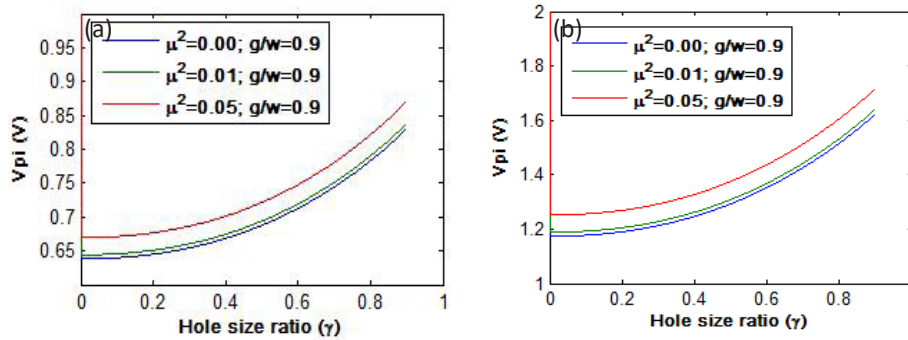


Fig. 3- Effect of hole size ratio γ on the pull-in voltage of perforated cantilever nanoswitch under (a) van der Waals force (b) Casimir force.

this effect is showed over the whole range of g/w . This confirm that the small scale effect increase the value of pull-in voltage, as shown in figure 2. These results confirm those presented in the work of Yang et al. [19] as well as those reported in refs [5, 18, 29, 30].

The pull-in voltage is plotted as a function of hole size ratio γ for value of gap ratio $g/w=0.9$ in figure 3. As can be seen, the pull-in voltage increases by increasing the value of γ , this due to the importance of the equivalent bending moment effect which decrease with γ . The change of pull-in voltage is noticed clearly compared the voltage of full-switch ($\gamma=0$) over the whole range of the section of nanocantilever beam.

Figure 4 shows the evolution of pull-in voltage as function of the number of holes N considering

the intermolecular force. A decrease in the pull-in voltage by increasing the number of holes N for different values of the nonlocal parameter μ due to the decrease of equivalent bending stiffness EI_{eq} which play a significant role when pull-in voltage occurs.

The results show that the pull-in voltage of perforated cantilever switch is more sensitive to the intermolecular force in the presence of Casimir force compared to the van der Waal force as indicated in Refs. [4, 5, 7, 19, 42-46, 50-51].

The variation of deflection is shown in figure 5 as function of γ including the small scale effect, it can be seen that the hole size ratio and gap ratio increase the cantilever pull-in deflection, this due to the reduction of active surface and the role of the equivalent bending moment effect.

Table 2- Comparison of the performance for NEMS switch reported in literature

Reference	Actuation voltage (V)	Switching time (μ s)
[49]	20	20,000-50,000
[47]	40	230
[48]	<8	<75
This research	5	<30

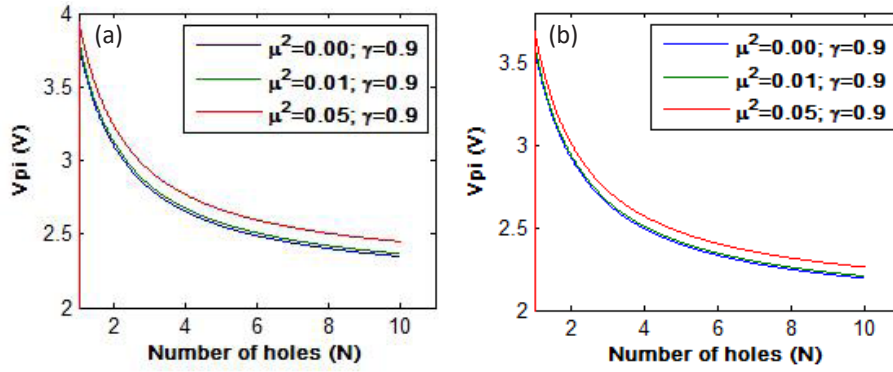


Fig. 4- Effect of number of holes N on the pull-in voltage of perforated cantilever nanoswitch under (a) van der Waals force (b) Casimir force.

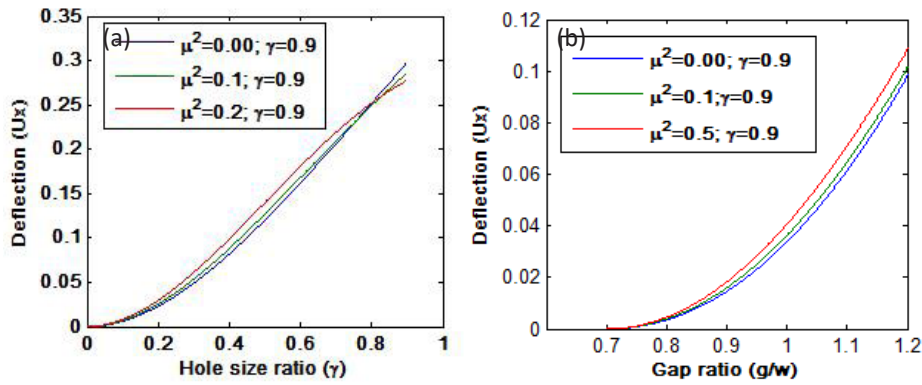


Fig. 5- Effect of hole size ratio γ on the pull-in deflection of perforated cantilever nanoswitch.

Comparing figure 4 and figure 5 reveals that the pull-in deflection is less sensitive to the hole size ratio and number of holes in comparison with the pull-in voltage.

6. Comparison of the Performance

Switching-on time is determined by the duration from a time when the pull-in voltage of the cantilever nano switch attained to the time when the state of the structure changed to be ON, as indicated in figure 6 which shows the result of the switching-on time of the proposed cantilever perforated nanoswitch.

As shown in figure 6, the switching-on time of the proposed structure is about 25 μ s. During the pull-in process, when the actuation voltage attains to 6V (the pull-in voltage), the driving of cantilever

begins to bend to the contact electrode. After 25 μ s, the circuit gets connected, and the voltage at both ends of the load reaches 5 V.

We observe that the operation speed of our device is faster than a conventional structure and the power consumption is lower than other devices and can rapidly switch between on and off states as indicated in table 2.

A comparison of the performance for NEMS switch reported in literature and in this research is done in Table 2 below.

From this table, we can conclude that the proposed NEMS in this research gives a lower actuation voltage (5 V) than the NEMS switch reported in the literature.

The actuation voltage and switching time performance show a certain degree of advantage.

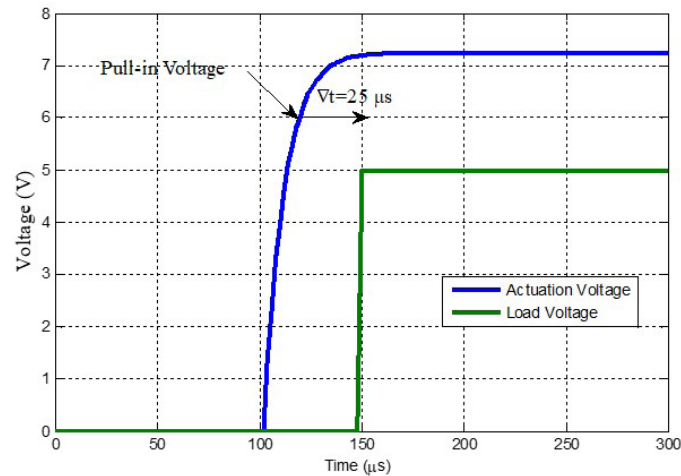


Fig. 6- Simulation of switching-on time of the proposed NEMS switch.

7. CONCLUSION

In this paper, the pull-in instability of a perforated cantilever nanoswitch with periodic square holes network has been studied in the presence of electrostatic and intermolecular forces. The deformation beam equation has been modified to include the electrostatic and intermolecular forces. The small scale effect is introduced by using the Eringen's nonlocal elasticity theory. LDL model has been applied to derive closed-form solutions for the critical pull-in parameters. The obtained results conclude that both hole size ratio γ and number of holes N reduce the pull-in voltage and thus perforated cantilever nanoswitches ($\gamma \neq 0$) are more sensitive to the dispersion force compared by full cantilever nanoswitches ($\gamma = 0$). It is found that the minimum initial gap rests insensitive to the nonlocal parameter while the pull-in parameters is increased when increasing its value which means that the small scale effect should be considered in the device design step. In addition, the perforated structure exhibits a good convergence when the analyzed number N is about ten holes or more per section. Therefore, the pull-in performance of cantilever nanoswitch under electrostatic and intermolecular forces can be modified geometrically by perforation procedure for a proper design with high sensitivity with respect to the conventional structure.

References

1. Kim P, Lieber CM. Nanotube Nanotweezers. *Science*. 1999;286(5447):2148-50.
2. Ponbunyanon P, Limkatanyu S, Kaewjuea W, Prachasaree W, Chub-Uppakarn T. A Novel Beam-Elastic Substrate Model with Inclusion of Nonlocal Elasticity and Surface Energy Effects.

- Arabic Journal for Science and Engineering. 2016;41(10):4099-113.
3. Wen-Hui L, Ya-Pu Z. Dynamic Behaviour of Nanoscale Electrostatic Actuators. *Chinese Physics Letters*. 2003;20(11):2070-3.
4. Lin WH, Zhao YP. Casimir effect on the pull-in parameters of nanometer switches. *Microsystem Technologies*. 2005;11(2-3):80-5.
5. Lin W, Zhao Y. Nonlinear behavior for nanoscale electrostatic actuators with Casimir force. *Chaos, Solitons & Fractals*. 2005;23(5):1777-85.
6. Vaghari M, Khayati GR, Jenabali Jahromi SA. Studying on the fatigue behavior of Al-Al₂O₃ metal matrix nano composites processed through powder metallurgy. *Journal of Ultrafine Grained and Nanostructured Materials*. 2019 Dec 31;52(2):210-7.
7. Ramezani A, Alasty A, Akbari J. Closed-form solutions of the pull-in instability in nano-cantilevers under electrostatic and intermolecular surface forces. *International Journal of Solids and Structures*. 2007;44(14-15):4925-41.
8. Ramezani A, Alasty A, Akbari J. Influence of van der Waals force on the pull-in parameters of cantilever type nanoscale electrostatic actuators. *Microsystem Technologies*. 2006;12(12):1153-61.
9. Rueckes T, Kim K, Joselevich E, Tseng GY, Cheung C-L, Lieber CM. Carbon Nanotube-Based Nonvolatile Random Access Memory for Molecular Computing. *Science*. 2000;289(5476):94-7.
10. Sahmani S, Bahrami M. Nonlocal plate model for dynamic pull-in instability analysis of circular higher-order shear deformable nanoplates including surface stress effect. *Journal of Mechanical Science and Technology*. 2015;29(3):1151-61.
11. J. Ntayeesh T, Rasheed Ismail M, G. Saihood R. Buckling analysis of reinforced composite plates with a multiwall carbon nanotube (MWCNT). *Periodicals of Engineering and Natural Sciences (PEN)*. 2019;7(3):1275.
12. Serry FM, Walliser D, Maclay GJ. The anharmonic Casimir oscillator (ACO)-the Casimir effect in a model microelectromechanical system. *Journal of Microelectromechanical Systems*. 1995;4(4):193-205.
13. Osterberg PM, Senturia SD. M-TEST: A test chip for MEMS material property measurement using electrostatically actuated test structures. *Journal of Microelectromechanical Systems*.

- 1997;6(2):107-18.
14. Bochobza-Degani O, Nemirovsky Y. Modeling the pull-in parameters of electrostatic actuators with a novel lumped two degrees of freedom pull-in model. *Sensors and Actuators A: Physical*. 2002;97-98:569-78.
 15. Ding J-N, Wen S-Z, Meng Y-G. Theoretical study of the sticking of a membrane strip in MEMS under the Casimir effect. *Journal of Micromechanics and Microengineering*. 2001;11(3):202-8.
 16. J. Israelachvili, (1991). Intermolecular and surface forces, 2nd edn. Academic. ISBN 0-12-375181-0 (Chapter 11).
 17. Lamoreaux SK. The Casimir force: background, experiments, and applications. *Reports on Progress in Physics*. 2004;68(1):201-36.
 18. Lu P, Lee HP, Lu C, Zhang PQ. Application of nonlocal beam models for carbon nanotubes. *International Journal of Solids and Structures*. 2007;44(16):5289-300.
 19. Yang J, Jia XL, Kitipornchai S. Pull-in instability of nano-switches using nonlocal elasticity theory. *Journal of Physics D: Applied Physics*. 2008;41(3):035103.
 20. Mousavi T, Bornassi S, Haddadpour H. The effect of small scale on the pull-in instability of nano-switches using DQM. *International Journal of Solids and Structures*. 2013;50(9):1193-202.
 21. Zeighampour H, Beni YT, Karimpour I. Torsional Vibration and Static Analysis of the Cylindrical Shell Based on Strain Gradient Theory. *Arabian Journal for Science and Engineering*. 2016;41(5):1713-22.
 22. A. C. Eringen, *Int. J. Eng. Sci.* 30 (10) (1992) 1551-1565.
 23. Kerid R, Bourouina H, Yahiaoui R, Bounekhla M, Aissat A. Magnetic field effect on nonlocal resonance frequencies of structure-based filter with periodic square holes network. *Physica E: Low-dimensional Systems and Nanostructures*. 2019;105:83-9.
 24. S. P. Timoshenko, J. M. Gere, 1961 *Theory of Elastic Stability* (New York McGraw Hill)
 25. Khan MU, Hassan G, Bae J. Non-volatile resistive switching based on zirconium dioxide: poly (4-vinylphenol) nanocomposite. *Applied Physics A*. 2019;125(6).
 26. Ansari R, Gholami R, Faghieh Shojaei M, Mohammadi V, Darabi MA. Surface Stress Effect on the Pull-In Instability of Hydrostatically and Electrostatically Actuated Rectangular Nanoplates With Various Edge Supports. *Journal of Engineering Materials and Technology*. 2012;134(4).
 27. Ghorbanpour Arani A, Ghaffari M, Jalilvand A, Kolahchi R. Nonlinear nonlocal pull-in instability of boron nitride nanoswitches. *Acta Mechanica*. 2013;224(12):3005-19.
 28. Wang KF, Wang BL, Zeng S. Small scale effect on the pull-in instability and vibration of graphene sheets. *Microsystem Technologies*. 2016;23(6):2033-41.
 29. Zeraati M, Khayati GR. Optimization of micro hardness of nanostructure Cu-Cr-Zr alloys prepared by the mechanical alloying using artificial neural networks and genetic algorithm. *Journal of Ultrafine Grained and Nanostructured Materials*. 2018 Dec 1;51(2):183-92.
 30. Soroush R, Koochi A, Kazemi AS, Noghrehabadi A, Haddadpour H, Abadyan M. Investigating the effect of Casimir and van der Waals attractions on the electrostatic pull-in instability of nano-actuators. *Physica Scripta*. 2010;82(4):045801.
 31. Taghavi N, Nahvi H. Pull-in instability of cantilever and fixed-fixed nano-switches. *European Journal of Mechanics - A/ Solids*. 2013;41:123-33.
 32. Keivani M, Mardaneh M, Koochi A, Rezaei M, Abadyan M. On the dynamic instability of nanowire-fabricated electromechanical actuators in the Casimir regime: Coupled effects of surface energy and size dependency. *Physica E: Low-dimensional Systems and Nanostructures*. 2016;76:60-9.
 33. Tomblor TW, Zhou C, Alexseyev L, Kong J, Dai H, Liu L, et al. Reversible electromechanical characteristics of carbon nanotubes under local-probe manipulation. *Nature*. 2000;405(6788):769-72.
 34. Bourouina H, Yahiaoui R, Kerid R, Ghomid K, Lajoie I, Picaud F, et al. The influence of hole networks on the adsorption-induced frequency shift of a perforated nanobeam using non-local elasticity theory. *Journal of Physics and Chemistry of Solids*. 2020;136:109201.
 35. Chan J, Eichenfield M, Camacho R, Painter O. Optical and mechanical design of a "zipper" photonic crystal optomechanical cavity. *Optics Express*. 2009;17(5):3802.
 36. Ding J-N, Wen S-Z, Meng Y-G. Theoretical study of the sticking of a membrane strip in MEMS under the Casimir effect-. *Journal of Micromechanics and Microengineering*. 2001;11(3):202-8.
 37. Frenzel T, Findeisen C, Kadic M, Gumbsch P, Wegener M. Tailored Buckling Microlattices as Reusable Light-Weight Shock Absorbers. *Advanced Materials*. 2016;28(28):5865-70.
 38. Nawaz H, Masood MU, Saleem MM, Iqbal J, Zubair M. Surface roughness effects on electromechanical performance of RF-MEMS capacitive switches. *Microelectronics Reliability*. 2020;104:113544.
 39. Lee W, Han H, Lotnyk A, Schubert MA, Senz S, Alexe M, et al. Individually addressable epitaxial ferroelectric nanocapacitor arrays with near Tb inch⁻² density. *Nature Nanotechnology*. 2008;3(7):402-7.
 40. J. W. N. Sharpe, R. Vaidyanathan, B. Yuan, G. Bao, R. L. Edwards, *J. Vacu. Sci. Techno. B* 15 (5) (1997) 1599-1603.
 41. Rabinovich VL, Gupta RK, Senturia SD. The effect of release-etch holes on the electromechanical behaviour of MEMS structures. *Proceedings of International Solid State Sensors and Actuators Conference (Transducers '97)*: IEEE.
 42. Luschi L, Pieri F. An analytical model for the determination of resonance frequencies of perforated beams. *Journal of Micromechanics and Microengineering*. 2014;24(5):055004.
 43. Luschi L, Pieri F. An analytical model for the resonance frequency of square perforated Lamé-mode resonators. *Sensors and Actuators B: Chemical*. 2016;222:1233-9.
 44. Ouakad HM. Numerical model for the calculation of the electrostatic force in non-parallel electrodes for MEMS applications. *Journal of Electrostatics*. 2015;76:254-61.
 45. Keivani M, Koochi A, Sedighi HM, Abadian A, Abadyan M. A Nonlinear Model for Incorporating the Coupled Effects of Surface Energy and Microstructure on the Electromechanical Stability of NEMS. *Arabian Journal for Science and Engineering*. 2016;41(11):4397-410.
 46. Rahmani O, Jandaghian AA. Buckling analysis of functionally graded nanobeams based on a nonlocal third-order shear deformation theory. *Applied Physics A*. 2015;119(3):1019-32.
 47. Song Y-H, Han C-H, Kim M-W, Lee JO, Yoon J-B. An Electrostatically Actuated Stacked-Electrode MEMS Relay With a Levering and Torsional Spring for Power Applications. *Journal of Microelectromechanical Systems*. 2012;21(5):1209-17.
 48. Li H, Ruan Y, You Z, Song Z. Design and Fabrication of a Novel MEMS Relay with Low Actuation Voltage. *Micromachines (Basel)*. 2020;11(2):171.
 49. Wong JE. *Analysis, design, fabrication, and testing of a MEMS switch for power applications* (Doctoral dissertation, Massachusetts Institute of Technology).
 50. Bourouina H, Yahiaoui R, Kerid R, Amine Benamar ME, Brioua F. Mathematical model for the adsorption-induced

nonlocal frequency shift in adatoms-nanobeam system. *Physica B: Condensed Matter*. 2017;520:128-38.

51. Ansari F, Sheibani S, Caudillo-Flores U, Fernández-García M. Effect of calcination process on the gas phase photodegradation by CuO-Cu₂O/TiO₂ nanocomposite photocatalyst. *Journal*

of Ultrafine Grained and Nanostructured Materials. 2020 Jun 1;53(1):23-30.

52. Yang Y, Lim CW. Non-classical stiffness strengthening size effects for free vibration of a nonlocal nanostructure. *International Journal of Mechanical Sciences*. 2012;54(1):57-68.